Environmental Science & Technology
Article
pubs.acs.org/est

In Situ Measurement of Dissolved Methane and Carbon Dioxide in Freshwater Ecosystems by Off-Axis Integrated Cavity Output Spectroscopy

Rodrigo Gonzalez-Valencia,[†] Felipe Magana-Rodriguez,[†] Oscar Gerardo-Nieto,[†] Armando Sepulveda-Jauregui,[‡] Karla Martinez-Cruz,[†,‡] Katey Walter-Anthony,[‡] Doug Baer,[§] and Frederic Thalasso*,[†,‡]

[†]Biotechnology and Bioengineering Department, Cinvestav, Avenida IPN 2508, Mexico City, San Pedro Zacatenco, D.V. 07360, Mexico

[‡]Water and Environmental Research Center, University of Alaska Fairbanks, Fairbanks, Alaska 07360, United States

[§]Los Gatos Research, Inc., Mountain View, California 94041, United States

Supporting Information

ABSTRACT: A novel low-cost method for the combined, real-time, and in situ determination of dissolved methane and carbon dioxide concentrations in freshwater ecosystems was designed and developed. This method is based on the continuous sampling of water from a freshwater ecosystem to a gas/liquid exchange membrane. Dissolved gas is transferred through the membrane to a continuous flow of high purity nitrogen, which is then measured by an off-axis integrated cavity output spectrometer (OA-ICOS). This method, called M-ICOS, was carefully tested in a laboratory and was subsequently applied to four lakes in Mexico and Alaska with contrasting climates, ecologies, and morphologies. The M-ICOS method allowed for the determination of dissolved methane and carbon dioxide concentrations with a frequency of 1 Hz and with a method detection limit of 2.76×10^{-10} mol L^{-1} for methane and 1.5×10^{-7} mol L^{-1} for carbon dioxide. These detection limits are below saturated concentrations with respect to the atmosphere and significantly lower than the minimum concentrations previously reported in lakes. The method is easily operable by a single person from a small boat, and the small size of the suction probe allows the determination of dissolved gases with a minimized impact on shallow freshwater ecosystems.

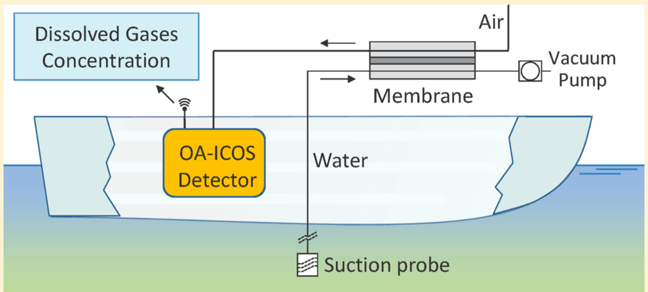

1. INTRODUCTION

Methane (CH_4) is a potent greenhouse gas that contributes about 20% of the warming induced by greenhouse gases.[1] An important fraction of CH_4 emissions comes from natural sources, and it has been estimated that natural ecosystems emit approximately 160 Tg CH_4 yr^{-1}.[2] Within these levels, it is estimated that lakes and reservoirs emit about 92 Tg CH_4 y^{-1}.[3]

CH_4 emissions from lakes and reservoirs depend on numerous processes involved in biogeochemical carbon cycling. For instance, the balance of CH_4 production by methanogens vs CH_4 oxidation by methanotrophs, two major counteractive processes, strongly control dissolved CH_4 concentrations in lake water.[4,5] Quantification of the resulting dissolved CH_4 concentration (C_{CH4}) throughout the water column is an important step in understanding the complexity of CH_4 cycling in freshwater ecosystems. Quantification of C_{CH4} ultimately allows the quantification of total diffusive CH_4 emissions to the atmosphere[6,7] or can be used as a pollution indicator.[8] Overall, C_{CH4} in lakes ranges usually from 1.00×10^{-8} to 3.00×10^{-3} mol L^{-1}.[9] This is more than C_{CH4} in equilibrium with atmospheric CH_4, which varies between 2.6×10^{-9} and 4.00×10^{-9} mol L^{-1}.[10−12]

The determination of dissolved CO_2 (C_{CO2}) is equally important, even if CO_2 emissions from freshwater ecosystems are often low compared to CH_4 emissions.[13] CO_2 is a central molecule of the carbon cycle, since it is the product of most biogeochemical processes, both aerobic and anaerobic, and the carbon source of several autotrophic processes, including primary production. Additionally, C_{CO2}, combined with other parameters, gives valuable information about bioprocesses occurring in an ecosystem. This is, for instance, the case of the respiratory quotient (Rq)[14] and of the ratio between CO_2 and CH_4 concentrations,[15] both being indicators of aerobic/anaerobic processes.

Received: February 26, 2014
Revised: September 10, 2014
Accepted: September 10, 2014

dx.doi.org/10.1021/es500987j | *Environ. Sci. Technol.* XXXX, XXX, XXX−XXX

Several methods have been used to measure C_{CH4} and C_{CO2} since the early 1960s.[16] The main methods that focus on dissolved CH_4 have been listed in detail.[17] Most of these methods are based on water/gas equilibration, followed by gas phase measurement, since gases are often poorly soluble in water; therefore, the water/gas equilibrium favors the latter. Additionally, most gases are easier to detect in the gas phase than dissolved in liquids. After the dissolved gas has been transferred to the gas phase, several detection methods have been used. These include standard gas chromatography,[18] mass spectrometry,[19] and laser based detectors, including tunable diode laser absorption spectroscopy.[9] Recently, significant advances have been made in the field of in situ quantification of dissolved gases, using underwater mass spectrometers[20] and off axis integrated cavity output spectrometers (OA-ICOS).[21] With the latter, the authors reported the novel application of an underwater OA-ICOS detector for the in situ measurement of dissolved CH_4 concentrations and isotopic compositions in the deep ocean. This method is now commercially available (Los Gatos Research Inc., Mountain View, CA).

These in situ methods represent a major breakthrough in the field and have a strong potential for application in challenging environments, such as the deep ocean. However, these methods are relatively expensive, require a remotely operated vehicle or a large frame, and have a response time of several minutes. In addition, at present, spectroscopic data analysis is performed off-line, not in real time, after the data is transferred to an external computer. Their application to freshwater ecosystems, which present a unique set of challenges, seems difficult in their current configuration. Freshwater ecosystems are often shallow; relatively small; located in remote locations; and morphologically complex, uneven, and variable relative to deep water bodies.[22] In such environments, a low-cost, lightweight, low-power, fast-response and simple-to-use detector, operable from a small boat, and based on a miniature probe to avoid environmental perturbation would represent a significant improvement to the previously reported methods. Furthermore, as freshwater ecosystems are subject to high spatial and temporal variations,[23,24] a high data acquisition rate, short response time, real-time data reporting, and wide dynamic range are additional requirements for correct and detailed appraisals in these diverse and complex ecosystems.

The objective of the present work is to develop and deploy a low-cost in situ detector for the combined measurement of C_{CH4} and C_{CO2}, based on an ultraportable OA-ICOS analyzer. As shown hereafter, this method employs a membrane gas/liquid exchange module. It was developed and tested in the laboratory, before field-testing in subtropical (Mexico) and boreal and tundra lakes (Alaska) with contrasting climates, ecologies, and morphologies. We demonstrate high data acquisition frequency and the precision and accuracy of the method.

2. MATERIALS AND METHODS

2.1. Detector and Prototype. We used an OA-ICOS ultraportable greenhouse gas analyzer (UGGA, model 915-0011, Los Gatos Research Inc.A) to detect and quantify CH_4, CO_2, and water vapor. This analyzer is ultraportable (essentially crushproof package and 15 kg weight), battery operated (70 W), and includes an internal vacuum pump for gas sampling, with a characteristic response time (time required to reach steady-state readings) of approximately 8 s. Details on the UGGA are presented in the Supporting Information (SI).

The UGGA was remotely operated and controlled from a tablet computer. The prototype was based on the transfer of the dissolved gases from a water sample to a gas phase, followed by the analysis of the gas phase by the UGGA. With this purpose, the prototype included a continuous flow of CH_4- and CO_2-free analytical grade nitrogen (Infra, Mexico or Airgas), controlled by a mass flow controller (GFC17, Aalborg) and a continuous flow of water extracted at the desired depth from the freshwater ecosystems through a vacuum line (Figure 1). The gas and the liquid crossed at a gas exchange station that will be described below. The liquid flow rate was controlled through a volumetric flask and by the measurement of the time required for the water sample to reach the gas exchange station. Details on the prototype are presented in the SI.

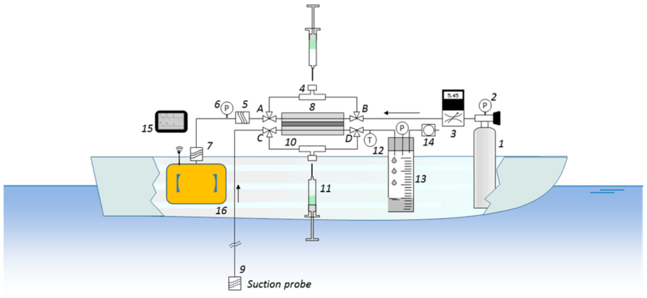

Figure 1. Prototype for dissolved CH_4 and CO_2 concentration measurements: 1. CH_4 free nitrogen; 2. pressure control; 3. mass flow controller; 4. septum port for gas sampling/injection; 5. membrane filter; 6. vacuum control; 7. additional membrane filter; 8. gas/liquid exchange module; 9. water filter; 10. water sampling port; 11. disposable syringe for water sampling and headspace injection; 12. temperature measurement; 13. liquid recollection tank with volume control; 14. portable vacuum pump; 15. tablet remote operation of the detector; 16. Ultraportable greenhouse gas analyzer; A, B, C, D. flow control 3-way valves.

To allow for easy field calibration, the prototype was used with two different modes of operation. The first, headspace equilibration combined with ICOS (H-ICOS), was a discrete sample measurement method, adapted from the traditional gas/liquid equilibration technique. While the water line was continuously operating, a 60 mL water sample from the desired depth was taken with a 60 mL disposable syringe from the water sampling port no. 10 (Figure 1). The sample was evacuated and replaced by a fresh sample. Then, 20 mL of the liquid content of the syringe was evacuated and replaced by CH_4- and CO_2-free nitrogen, taken from septum port no. 4. The gas and liquid volumes were recorded, and the syringe was vigorously shaken for 20 s to allow for gas/liquid equilibration. Then, 15 mL of the 20 mL headspace of the syringe was injected in the gas line through port no. 4. The injection of that sample in the gas line caused a peak response (in ppm) of the UGGA that was integrated to determine the headspace CH_4 and CO_2 concentrations, in a way similar to, for instance, standard gas chromatography methods. After injecting the headspace sample in the UGGA, the temperature of the water sample in the syringe was determined, and the dissolved gas concentration in the original water sample was determined according to Henry's law (SI Equations S1 and S2).

The second method, membrane combined with ICOS (M-ICOS), was a continuous measurement method that consisted of a counter flow of CH_4- and CO_2-free nitrogen and water continuously extracted by a vacuum pump at the desired depth, crossing in a Permselect module (PDMSXA-1000, Medarray Inc.; Figure 1, no. 8). This exchange module was composed of an array of approximately 1250 silicone hollow fibers of 190 μm internal diameter, 55 μm thickness, with a total exchange area of 1000 cm^2. The water flowed outside of the hollow fibers, inside the module's shell, while the CH_4- and CO_2-free nitrogen flowed inside the hollow fibers. Because of diffusive forces, the dissolved CH_4 and CO_2 contained in the water were transferred to the gas phase, where they were detected by the UGGA.

The gas transfer can be described by a diffusion model according to Fick's second law (eq 1), where dM/dt is the mass transfer rate (mol s^{-1}); 1000 is a unit conversion factor from mol L^{-1} to mol m^{-3}; K is the membrane transfer coefficient (m s^{-1}); A_M is the area of the membrane (m^2); C_w is the dissolved gas concentration in the water sample (CH_4 or CO_2; mol L^{-1}); C_g is the gas concentration in the gas phase (mol L^{-1}); and H' is the CH_4 and CO_2 air/water partition coefficient (−), defined from SI eq S2.

$$\frac{dM}{dt} = 1000 \cdot K \cdot A_M \cdot \left(C_w - \frac{C_g}{H'} \right) \tag{1}$$

As shown in the SI, a direct proportionality between C_w and C_g can be established from eq 1, giving eq 2, where α (dimensionless) is the proportionality parameter combining all membrane, gas, and water transfer characteristics (Q_g, K, A_M and H'), for an easier calculation.

$$C_w = C_g \cdot \alpha \tag{2}$$

The parameter α can be determined by measuring first C_w by the H-ICOS method and then, with the same sample, by measuring C_g by the M-ICOS. This can be easily done in the field with actual water samples.

The M-ICOS method is subject to a delay time (t_d) between the time that the sample is actually extracted and the time that it reaches the gas/liquid module, where it is measured. Furthermore, there is an additional response time corresponding to the time required to reach steady-state readings at the UGGA. As will be shown in the Results section, a continuous flow stirred tank reactor (CSTR) model of hydraulic residence time[25] describes the hydraulic behavior of the system (eq 3) well, where C_{wm} is the dissolved gas concentration measured in the water (mol L^{-1}) and t_r is the response time of the system, which can be also taken as the hydraulic residence time of the prototype.

$$C_{wm} = C_w \cdot \left[1 - \exp\left(-\frac{t}{t_r} \right) \right] \tag{3}$$

After derivation of eq 3, eq 4 shows that online and real-time measurement of C_w can be obtained, thus avoiding long delay times between samples (see SI for details).

$$C_{w,t} = \frac{dC_{wm,t+t_d}}{dt} \cdot t_r + C_{wm,t+t_d} \tag{4}$$

2.2. Laboratory Testing. The laboratory testing of both H-ICOS and M-ICOS methods is described in detail in the SI. Briefly, we tested the precision and linearity of the UGGA by injecting several CH_4 and CO_2 standards and by determining the signal-to-noise ratio at several gas concentrations. We then tested the H-ICOS concept by establishing the peak response of the UGGA to several volumes and CH_4 and CO_2 concentrations injected in the gas line. Next, synthetic water samples with a known C_w were prepared in a lab-scale stirred tank reactor (STR) by injecting a continuous flow of standard gases in tap water with strong mixing (800 rpm), until saturation was reached. C_w in these water samples was theoretically established according to Henry's Law (SI eqs S1 and S2). With these water samples, we established the time necessary to reach equilibrium between the water sample and the headspace of the sampling syringe, which is a basic requirement of the H-ICOS method. We also tested the H-ICOS method by comparing the measured C_w to the theoretical concentrations. We used the same samples to test the M-ICOS method. Measurements completed with the M-ICOS method were also compared to the theoretical concentrations, and the parameter α was determined. The t_d and t_r of the M-ICOS method were established by switching between water containing CH_4 and CO_2, and degassed water using a 3-way valve. These experiments were used to check the developed t_r model (eq 4).

2.3. Field-Testing. In order to validate the method in real case scenarios and to provide a demonstration of how the instrument operates under a range of field conditions, the prototype and both methods were tested in four lakes with contrasting climates, ecologies, and morphologies: (i) a eutrophic subtropical reservoir located in the Mexico metropolitan area (Lake Guadalupe); (ii) a mesotrophic subtropical reservoir located in the same drainage basin as Lake Guadalupe (Lake Llano); (iii) a shallow Alaskan thermokarst lake located in the boreal zone (Lake Goldstream); and (iv) a shallow nonthermokarst Alaskan lake located in the tundra (Lake Otto). Field studies were done in July 2013 (Lake Guadalupe and Lake Llano) and in August 2013 (Lake Otto and Lake Goldstream). In all lakes, C_w profiles were determined by the M-ICOS method after determination of α with the H-ICOS method (see Results and Discussion section). The profile procedure that best worked was as follows: the probe was maintained a few centimeters below the water surface for about 30 s; then the probe was lowered slowly and steadily by hand to the bottom of the lake, where it was maintained for an additional 30 s. A controlled diving speed was maintained, and to know the approximate depth corresponding to each concentration data, the time at each 0.5 m intermediary depths was noted. The diving speed was about 0.6 m min^{-1}. With this procedure, about 100 data were acquired for each m of water column depth. The C_w data were corrected according to eq 4 before being interpreted.

We also measured in each lake the dissolved oxygen (DO) and pH profiles with a multiparametric probe (YSI 556 MPS, YSI, Yellow Springs, OH, in Mexico or Hydrolab Data Sonde, Hach Hydromet, Loveland, CO, in Alaska). Rq, expressed as the ratio between CO_2 production and O_2 consumption (mol mol^{-1})[26] was determined according to eq 5,[15] where C^*_{CO2} and DO* are the CO_2 and DO concentration in equilibrium with the atmosphere.

$$\mathrm{Rq} = \frac{C_{CO2} - C^*_{CO2}}{\mathrm{DO}^* - \mathrm{DO}} \tag{5}$$

3. RESULTS AND DISCUSSION

3.1. Laboratory Testing. The injection of several standard gases from 2 to 500 ppm of CH_4 and 20 to 1500 ppm of CO_2 in the UGGA showed that the latter did not require further calibration, apart from its original factory calibration. The

UGGA gave a linear response in the entire range tested. The signal-to-noise ratio, measured over 10 min for all standard gases, was 1520 ± 415 for CH_4 and 1803 ± 344 for CO_2. We tested the peak response of the UGGA to the injection of several CH_4 and CO_2 quantities, which is the core concept of the H-ICOS method. SI Figure S1A shows an example of the UGGA response to the triplicate injection of 5 mL nitrogen, containing 2 ppm of CH_4, which corresponds to an injected quantity of 4.31×10^{-10} mol. SI Figure S1B indicates the linear response of the UGGA to a range of 8.31×10^{-12} to 1.63×10^{-8} mol CH_4 and to a range of 2.61×10^{-9} to 1.33×10^{-6} mol CO_2. The linear response of the UGGA for both gases indicated the validity of CH_4 and CO_2 quantification by peak injections. With these results, we estimated the method detection limit (MDL),[27] of the H-ICOS method. The minimum CH_4 quantity that was distinguishable from background noise with 99% confidence was 7.63×10^{-12} mol. An example of UGGA response to that CH_4 quantity is shown in inner SI Figure S1A. By using eqs 1 and 2 and under the experimental conditions, this MDL corresponds to a C_{CH4} of 2.69×10^{-10} mol L^{-1}. This MDL is significantly lower than the range of C_{CH4} reported in lakes[9] and about 35 times less than the minimum C_{CH4} concentration of 1.00×10^{-8} mol L^{-1} among the lowest C_{CH4} reported.[11,28,29] This detection limit is also significantly lower than the C_{CH4} at equilibrium with atmospheric CH_4, which is 2.80×10^{-9} mol L^{-1} (SI eq S1) at 20 °C and with 1.8 ppm atmospheric CH_4.[30] The same procedure revealed the MDL of C_{CO2} measurements as 2.39×10^{-7} mol L^{-1}. This MDL is less than the lower range reported in lakes; 1.00×10^{-5} and 1.30×10^{-5} mol L^{-1}.[31,32] This CO_2 MDL is also significantly lower than the dissolved concentration in equilibrium with atmospheric CO_2, which is 1.54×10^{-5} mol L^{-1} (SI eq 1) at 20 °C and with 390 ppm atmospheric CO_2.[30] We did not test the maximum C_w that could be measured by the H-ICOS method. According to SI eqs S1 and S2, the volume of headspace injected can be reduced with no theoretical limit in order to avoid the injection of an excessive gas quantity to the UGGA.

The H-ICOS method depends on reaching equilibrium between the water phase and the gaseous headspace in a sampling syringe. The effect of the shaking time on the water/liquid equilibration was determined using water samples prepared in the STR containing known C_{CH4} and C_{CO2}. The water samples were gently taken, complemented with CH_4- and CO_2-free nitrogen, and vigorously shaken for 0 to 30 s, prior to the headspace injection into the UGGA. SI Figure S2 shows the results obtained, where dissolved gas concentrations are normalized, 1.0 being the final equilibrium concentration. As shown, 10 to 15 s were required to reach equilibrium. According to these results, a shaking time of 20 s was used thereafter as a standard operating procedure.

The H-ICOS method was also tested in the laboratory, under simulated field-conditions; that is, using the prototype and sampling water prepared in the STR, which contained several values of C_w. Figure 2 shows the correlation between the measured and theoretical C_{CH4} (determined from SI eq 1). A linear response was observed. Similar results were obtained with C_{CO2} (results not shown). The standard error of the mean (see SI) was estimated to 2.15% for C_{CH4} and to 1.45% for C_{CO2} for triplicates.

During the same experiment, the water extracted from the STR was also measured by the M-ICOS method. By comparing the M-ICOS readings with theoretical C_{CH4}, α was determined to be 8.87 ± 0.30 (eq 2). Figure 2 shows the C_{CH4} determined by the M-ICOS, according to that α. For CO_2, α was 23.97 ± 1.98 (results no shown). During these M-ICOS determinations, the standard error of the mean was 0.17% for C_{CH4} and 0.20% for C_{CO2} for a sampling period of 100 s. Remembering that the parameter α relates the gas concentration read by the UGGA and the actual C_{CH4}, this allows the determination of the MDL of the M-ICOS method. Assuming a MDL of the UGGA of 1 ppb for CH_4 and 200 ppb for CO_2, which correspond to 4.19×10^{-11} and 8.41×10^{-9} mol L^{-1} at atmospheric pressure and 20 °C, respectively, the M-ICOS method would have a MDL of 2.76×10^{-10} mol L^{-1} for C_{CH4} and of 1.50×10^{-7} mol L^{-1} for C_{CO2}. These MDL are similar to those estimated for the H-ICOS method and are lower than the dissolved concentration in equilibrium with atmospheric CH_4 and CO_2.

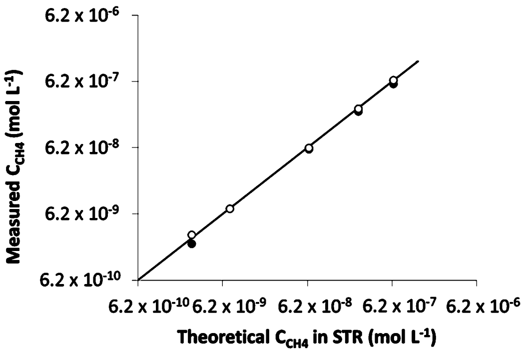

Figure 2. Measured C_{CH4} by H-ICOS (white dots) and by M-ICOS (black dots) vs. theoretical C_{CH4} concentration prepared in a stirred tank reactor. Straight line shows the observed correlations (slope = 1).

To validate the developed response time model (eq 4), several tests were done with different tubing lengths and different gas and liquid flow rates. SI Figure S3 shows an example of the response of the M-ICOS method to sudden change in water concentrations. The model fitted well the experimental data (R^2 for 10 tests = 0.996 ± 0.004), which allowed, after data processing, the determination of C_w from C_{wm} data, which is a requirement for online measurements.

3.2. Field-Testing.

In the field, the H-ICOS and the M-ICOS methods were tested to assess their operability and also to determine the α parameter. The H-ICOS method required approximately 3 min per measurement. Triplicate H-ICOS measurements at the same locations and depths of the Lake Guadalupe gave a standard error of the mean of 3.40% for CH_4 and 2.59% for CO_2. This error was greater than the error observed during laboratory testing (2.15% and 1.45% for C_{CH4} and C_{CO2}, respectively), probably because the water samples were independent and taken from slightly different locations because of boat motion. The M-ICOS readings were compared to the C_{CH4} and C_{CO2} measurements completed with the H-ICOS method, in order to determine the α parameter. The α parameter was measured at several depths of each lake to take into account possible differences in temperature and the concentration of dissolved gas. In different lakes and for CH_4, α ranged from 8.05 to 10.73 with a coefficient of variation (see SI) of 9.4%, whereas for CO_2, α ranged from 19.17 to 33.11 with a coefficient of variation of 23.5%. These relatively large variations are easily explained by the complexity of α, which depends on Q_g, K, and H'. In turn, K and H' depend on the temperature of the water and the gas phase, with complex heat transfer between them. However, by comparing α measured within a given lake and maintaining fixed gas and liquid flow rates, the coefficient of variation of α was reduced to 7.9% for CH_4 and 13.9% for CO_2. In Lake Guadalupe and Lake Llano, which are relatively deep and were thermally stratified, the correlation between α and temperature was tested. No trend was observed, probably because of the relatively small temperature gradient (2.7 °C in both cases). However, for the future application of the method in lakes with high thermal stratification, we advise the determination of α at several depths of the lakes, for potential temperature compensation.

Additionally, t_d and t_r were tested in each lake. This was done by rapidly (about 1−2 s) submerging the probe from the surface, where C_{CH4} was usually low, to a greater depth, where C_{CH4} was usually higher. SI Figure S4 shows an example of the field response of the M-ICOS method to sudden change in water concentrations in Lake Guadalupe, as well as C_{CH4} calculated from eq 4. This strategy allowed the field determination of t_d and t_r. As expected, t_d depended on the length of the tubing and the liquid flow rate, while t_r depended on the gas and liquid flow rates. Little or no effect of tubing length (varying from 6 to 20 m) on t_r was observed. The concentration profiles vs. time were similar to those observed in the laboratory (SI Figure S3) and fitted well the developed model (eq 4). It was observed that both t_d and t_r were stable for fixed gas and liquid flow rates, changing only a few percent over time. From this observation, we decided to determine t_r and t_d only every three C_w profiles. In Lake Goldstream, the diameter of the particulate matter was visually larger than in the other lakes and generated a clogging of the suction probe, i.e. an increase in t_d, during some measurements of the suction probe was observed. In that lake, after each profile, the cleanliness of the probe filter was visually checked, and if dirt had accumulated, t_d was measured before validating the previous profile, or alternatively, the filter was washed and the profile repeated.

The M-ICOS method was tested to determine C_w profiles. Figure 3 shows an example of the triplicate C_{CH4} and C_{CO2} profiles that were obtained sequentially in Lake Guadalupe at the same location. The three determinations gave similar profiles, with lower C_{CH4} and C_{CO2} concentrations in superficial water than bottom water, as often observed in lakes.[33−35] A strong C_{CH4} gradient was observed in Lake Guadalupe between 2.5 and 5 m depth, with an average of $7.57 \times 10^{-5} \pm 7.10 \times 10^{-6}$ mol L^{-1} (mean ± sd). Above 2.5 m, C_{CH4} was lower ($1.95 \times 10^{-6} \pm 5.43 \times 10^{-7}$ mol L^{-1}) probably due to a combined effect of atmospheric exchange and the presence of DO, which probably promoted CH_4 oxidation (Figure 4 A). A similar C_{CO2} gradient was observed between 1.0 to 5.0 m depth. By comparing the three profiles, the arithmetic mean of the relative error (relative difference between measurements done at the same depth) was 11.15% for C_{CH4} and 8.1% for C_{CO2}. The error was significantly higher when C_w changed abruptly in the ecosystem. For instance, the mean C_{CH4} error was 56.7% at depths between 2.5 and 3.3 m (Figure 3C), while it was 5.3% outside that depth range. The latter was attributed to error in depth measurements, and a further improvement of the M-ICOS method would involve the coupling of a depth sensor to the suction probe.

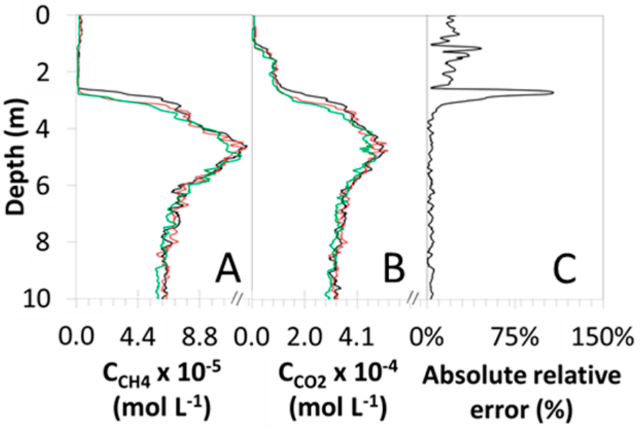

Figure 3. Example of triplicate C_{CH4} (A) and C_{CO2} (B) profiles measured in Lake Guadalupe and absolute relative error between triplicate measurements of C_{CH4} (C).

Figure 4 shows the depth profiles for C_{CH4} and C_{CO2} in the four lakes. In all lakes, except Lake Otto (Figure 4D), clear C_{CH4} and C_{CO2} gradients were observed. The absence of C_{CH4} and C_{CO2} gradients in Lake Otto can be explained by the fact that Lake Otto is a shallow nonthermokarst lake, classified as oligotrophic,[36] which indicates a low organic carbon input and, therefore, a low methanogenic potential. Additionally, Lake Otto is a lake exposed to constant winds and is therefore well mixed and oxygenated. Contrastingly, steep gradients were observed in Lake Guadalupe (Figure 4A) and in Lake Goldstream (Figure 4C), which receive high carbon input from pollution and thawing permafrost,[37] respectively. It is noticeable that Lake Llano (Figure 4B), which is an unpolluted lake in the same drainage basin as Lake Guadalupe, exhibited moderate gradients. Combined with the DO profiles, also shown in Figure 4, it is clear that when C_{CH4} and C_{CO2} gradients were observed, the trend was opposite to that of the DO profile, particularly in the oxycline.

These results confirm that the M-ICOS method allowed the determination of high-resolution C_w profiles. To the best of our knowledge, this is the first time a method that allows the determination of combined C_{CH4} and C_{CO2} data at a frequency of 1 Hz has been reported. In addition, the M-ICOS, allows the determination of the ratio between both parameters, which is an indication of the major processes involved in carbon cycling. CH_4 is mainly produced by strict anaerobic methanogenesis and consumed by methanotrophy, while CO_2 is a product of both anaerobic and aerobic metabolic processes. Thus, the ratio between C_{CH4} and C_{CO2} is an indication of aerobic vs. anaerobic organic carbon utilization. Figure 4 shows the C_{CH4}/C_{CO2} ratios observed in the four lakes. In Lake Guadalupe and Lake Goldstream (Figures 4A and 4C, respectively), a step gradient was observed, just below the oxycline, while in Lake Llano, a moderate gradient was observed; no gradient was observed in Lake Otto. The M-ICOS method is also a convenient tool for the determination of Rq, which describes the predominance of anaerobic over aerobic metabolism.[15] Figure 4 shows the Rq profiles observed in the water column in the four lakes. No Rq gradient was observed in Lake Otto, while in Lake Llano, a moderate gradient was detected. However, in both lakes, the Rq was significantly lower than 1.0, which is indicative of aerobic processes. In Lake Guadalupe, a clear gradient was observed, and Rq values greater than 1.0 were seen below the oxycline, an indicator of the predominance of anaerobic metabolisms. In Lake Goldstream, the Rq was surprisingly high, with values ranging from 4.0 to 25.4; the higher values were observed in the aerobic epilimnion of the lake, contrarily to what is generally reported.[15,26,38,39] It should be pointed out that Lake

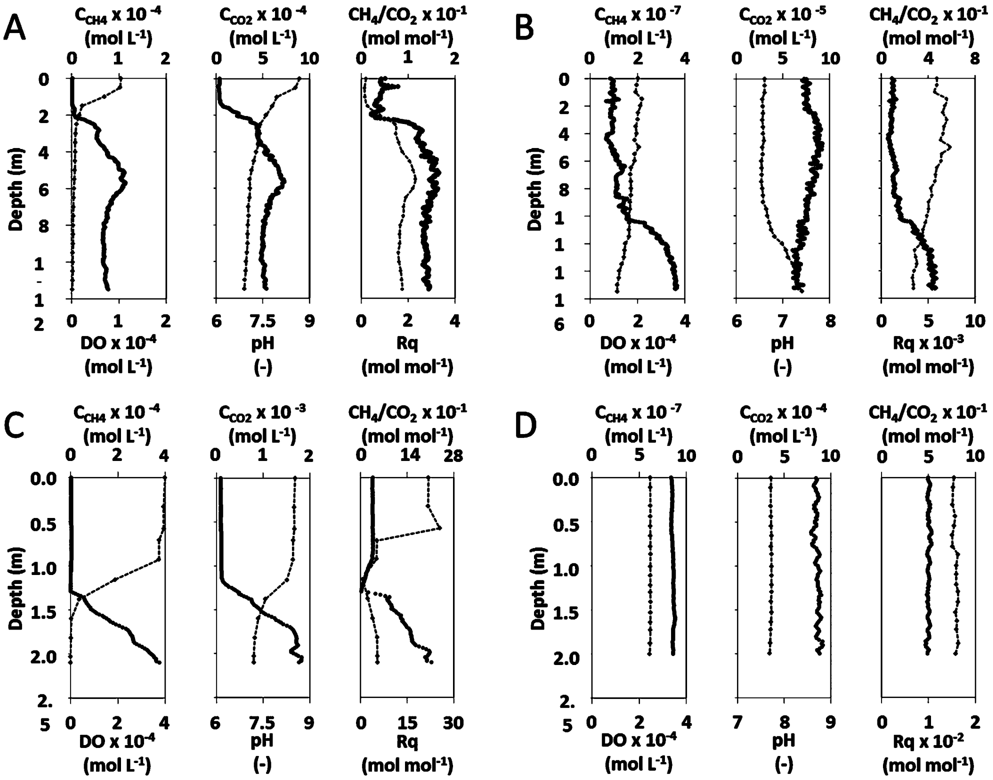

Figure 4. Profiles observed in Lake Guadalupe (A), Lake Llano (B), Lake Goldstream (C) and Lake Otto (D) of C_{CH4} (black dots), C_{CO2} (black dots), Dissolved oxygen (dotted line), pH (dotted line), CH_4/CO_2 (black dots), and Respiratory Quotient (dotted line). Note the different *y*- and *x*-axis scales among lakes.

Goldstream has been classified as a dystrophic lake (a brown-water yedoma lake with high dissolved organic carbon concentrations),[40] with high level of CO_2 emissions.[41] In order to obtain high frequency in Rq determinations, a further improvement of the M-ICOS method would require the combination of a high frequency DO sensor and the suction probe.

3.3. Comments and Recommendations. The M-ICOS prototype and method, combined with the H-ICOS method for field calibration, allowed the determination of C_w with a frequency of 1 Hz and with a MDL of 2.76×10^{-10} mol L^{-1} for C_{CH4} and of 1.50×10^{-7} mol L^{-1} for C_{CO2} (see SI Table S2 for specifications). These MDL are significantly lower than the minimum concentrations in lakes, as reported in the literature, and than the C_{CH4} and C_{CO2} of freshwater in equilibrium with the atmosphere. The small size of the suction probe (6 mm tubing) and the relatively low liquid flow rate required by the method (600 mL min^{-1}) allows for the determination of C_w with a minimized impact on the ecosystem, including shallow freshwater ecosystems, and with an accurate location and depth awareness.

A possible limitation of the method is the requirement of water sampling, making its application difficult at low air temperature (below freezing), when ice formation may be occurring at the waterline exposed to air. The method application in deep aquatic ecosystems could also be a limitation of the method. In the present work, the M-ICOS method was applied up to a maximum depth of 20 m. Its application in deeper ecosystems would increase t_d, which is a direct function of the length of the sampling tubing. Additionally, axial dispersion within the water flow in the sampling tubing would also certainly become important, resulting in a long t_r. The combined increase in t_d and t_r could be described by a more complex hydraulic residence time model, yielding no theoretical limit to the depth of measurement, despite its practice limitations. The application of the M-ICOS method in oceanographic sciences would present several bottlenecks, compared to the actual state of the art OA-ICOS method.[21] The first one is undoubtedly a very long delay time of several hours between sampling and measurement for depths greater than 1000 m, assuming the same liquid flow speed as observed in the present work. Compared to the 5 min response time reported,[20] these delays are extremely long and may require complex hydraulic flow modeling and an extremey low permeability sampling line. The second bottleneck is the MDL of the M-ICOS method, which is very close to the lower CH_4 concentration range reported in oceans, that is, in the low nmol L^{-1} range.[7]

Several further developments of the M-ICOS method are recommended. First, to couple the suction probe to a depth sensor and a fast DO sensor, which would allow for a more precise measurement of the C_{CH4} and C_{CO2} profiles and a high throughput Rq determination. Second, to use other OA-ICOS detectors to determine the dissolved concentration of analytes such as ammonia, nitrous oxide, oxygen and hydrogen sulfide. OA-ICOS detectors for each of these analytes are now commercially available. And third, a very significant advancement would be to combine our design prototype with stable isotope analyzers, currently available to determine even more specifically the turnover dynamics of different metabolically active and linked analytes.

■ ASSOCIATED CONTENT

Ⓢ Supporting Information

Extended experimental methods and figures. This material is available free of charge via the Internet at http://pubs.acs.org.

■ AUTHOR INFORMATION

Corresponding Author

*Phone: (52) 55 57 47 33 20; fax (52) 55 57 47 38 38; e-mail: thalasso@cinvestav.mx; fthalasso@alaska.edu.

Author Contributions

The manuscript was written through contributions of all authors. All authors have given approval to the final version of the manuscript

Notes

The authors declare no competing financial interest

■ ACKNOWLEDGMENTS

We gratefully acknowledge the financial support of Rodrigo Gonzalez-Valencia (grant no. 266244/219391), Felipe Magana-Rodriguez (grant no. 419562/261800), Oscar Gerardo-Nieto (grant no. 485051/277238), and Karla Martinez-Cruz (grant no. 330197/233369) by the Consejo Nacional de Ciencia y Tecnología. Support for fieldwork in Alaska was provided through DOE DE-SC0006920, NSF OPP no. 1107892, NASA no. NNX11AH20G. We also thank Mr. Joel Salinas and Mr. Efraín Maldonado, SCR Mexico, for their support in the acquisition of the material and equipment.

■ REFERENCES

(1) Kirschke, S.; Bousquet, P.; Ciais, P.; Saunois, M.; Canadell, J. G.; Dlugokencky, E. J.; Bergamaschi, P.; Bergmann, D.; Blake, D. R.; Bruhwiler, L.; Cameron-Smith, P.; Castaldi, S.; Chevallier, F.; Feng, L.; Fraser, A.; Heimann, M.; Hodson, E. L.; Houweling, S.; Josse, B.; Fraser, P. J.; Krummel, P. B.; Lamarque, J.-F.; Langenfelds, R. L.; Le Quere, C.; Naik, V.; O'Doherty, S.; Palmer, P. I.; Pison, I.; Plummer, D.; Poulter, B.; Prinn, R. G.; Rigby, M.; Ringeval, B.; Santini, M.; Schmidt, M.; Shindell, D. T.; Simpson, I. J.; Spahni, R.; Steele, L. P.; Strode, S. A.; Sudo, K.; Szopa, S.; van der Werf, G. R.; Voulgarakis, A.; van Weele, M.; Weiss, R. F.; Williams, J. E.; Zeng, G. Three decades of global methane sources and sinks. *Nat. Geosci.* **2013**, *6* (10), 813−823.

(2) Wuebbles, D. J.; Hayhoe, K. Atmospheric methane and global change. *Earth-Sci. Rev.* **2002**, *57* (3−4), 177−210.

(3) Bastviken, D.; Tranvik, L. J.; Downing, J. A.; Crill, P. M.; Enrich-Prast, A. Freshwater methane emissions offset the continental carbon sink. *Science* **2011**, *331* (6013), 50−50.

(4) Thauer, R. K.; Kaster, A. K.; Seedorf, H.; Buckel, W.; Hedderich, R. Methanogenic archaea: ecologically relevant differences in energy conservation. *Nat. Rev. Microbiol.* **2008**, *6* (8), 579−591.

(5) Tranvik, L. J.; Downing, J. A.; Cotner, J. B.; Loiselle, S. A.; Striegl, R. G.; Ballatore, T. J.; Dillon, P.; Finlay, K.; Fortino, K.; Knoll, L. B.; Kortelainen, P. L.; Kutser, T.; Larsen, S.; Laurion, I.; Leech, D. M.; McCallister, S. L.; McKnight, D. M.; Melack, J. M.; Overholt, E.; Porter, J. A.; Prairie, Y.; Renwick, W. H.; Roland, F.; Sherman, B. S.; Schindler, D. W.; Sobek, S.; Tremblay, A.; Vanni, M. J.; Verschoor, A. M.; von Wachenfeldt, E.; Weyhenmeyer, G. A. Lakes and reservoirs as regulators of carbon cycling and climate. *Limnol. Oceanogr.* **2009**, *54* (6), 2298−2314.

(6) Kling, G. W.; Kipphut, G. W.; Miller, M. C. The flux of CO_2 and CH_4 from lakes and rivers in arctic Alaska. *Hydrobiologia* **1992**, *240* (1−3), 23−36.

(7) Reeburgh, W. S. Oceanic methane biogeochemistry. *Chem. Rev.* **2007**, *107* (2), 486−513.

(8) Amos, R. T.; Mayer, K. U.; Bekins, B. A.; Deliln, G. N.; Williams, R. L. Use of dissolved and vapor-phase gases to investigate methanogenic degradation of petroleum hydrocarbon contamination in the subsurface. *Water Resour. Res.* **2005**, *41* (2), W02001.

(9) Sepulveda-Jauregui, A.; Martinez-Cruz, K.; Strohm, A.; Anthony, K. M. W.; Thalasso, F. A new method for field measurement of dissolved methane in water using infrared tunable diode laser absorption spectroscopy. *Limnol. Oceanogr. Meth.* **2012**, *10*, 560−567.

(10) Duchemin, E.; Lucotte, M.; Canuel, R. Comparison of static chamber and thin boundary layer equation methods for measuring greenhouse gas emissions from large water bodies. *Environ. Sci. Technol.* **1999**, *33* (2), 350−357.

(11) Huttunen, J. T.; Hammar, T.; Alm, J.; Silvola, J.; Martikainen, P. J. Greenhouse gases in non-oxygenated and artificially oxygenated eutrophied lakes during winter stratification. *J. Environ. Qual.* **2001**, *30* (2), 387−394.

(12) Kankaala, P.; Huotari, J.; Peltomaa, E.; Saloranta, T.; Ojala, A. Methanotrophic activity in relation to methane efflux and total heterotrophic bacterial production in a stratified, humic, boreal lake. *Limnol. Oceanogr.* **2006**, *51* (2), 1195−1204.

(13) Soumis, N.; Duchemin, E.; Canuel, R.; Lucotte, M. Greenhouse gas emissions from reservoirs of the western United States. *Global Biogeochem. Cycles* **2004**, *18* (3), GB3022.

(14) McNair, J. N.; Gereaux, L. C.; Weinke, A. D.; Sesselmann, M. R.; Kendall, S. T.; Biddanda, B. A. New methods for estimating components of lake metabolism based on free-water dissolved-oxygen dynamics. *Ecol. Model.* **2013**, *263*, 251−263.

(15) Richey, J. E.; Devol, A. H.; Wofsy, S. C.; Victoria, R.; Riberio, M. N. G. Biogenic gases and the oxidation and reduction of carbon in amazon river and floodplain waters. *Limnol. Oceanogr.* **1988**, *33* (4), 551−561.

(16) Swinnerton, J. W.; Cheek, C. H.; Linnenbom, V. J. Determination of dissolved gases in aqueous solutions by gas chromatography. *Anal. Chem.* **1962**, *34* (4), 483−485.

(17) Boulart, C.; Connelly, D. P.; Mowlem, M. C. Sensors and technologies for in situ dissolved methane measurements and their evaluation using Technology Readiness Levels. *Trac-Trend. Anal. Chem.* **2010**, *29* (2), 186−195.

(18) Jahangir, M. M. R.; Johnston, P.; Khalil, M. I.; Grant, J.; Somers, C.; Richards, K. G. Evaluation of headspace equilibration methods for quantifying greenhouse gases in groundwater. *J. Environ. Manage.* **2012**, *111*, 208−212.

(19) Schluter, M.; Gentz, T. Application of membrane inlet mass spectrometry for online and in situ analysis of methane in aquatic environments. *J. Am. Soc. Mass Spectrom.* **2008**, *19* (10), 1395−1402.

(20) Bell, R. J.; Short, R. T.; Van Amerom, F. H. W.; Byrne, R. H. Calibration of an in situ membrane inlet mass spectrometer for measurements of dissolved gases and volatile organics in seawater. *Environ. Sci. Technol.* **2007**, *41* (23), 8123−8128.

(21) Wankel, S. D.; Huang, Y. W.; Gupta, M.; Provencal, R.; Leen, J. B.; Fahrland, A.; Vidoudez, C.; Girguis, P. R. Characterizing the distribution of methane sources and cycling in the deep sea via in situ stable isotope analysis. *Environ. Sci. Technol.* **2013**, *47* (3), 1478−1486.

(22) Downing, J. A.; Prairie, Y. T.; Cole, J. J.; Duarte, C. M.; Tranvik, L. J.; Striegl, R. G.; McDowell, W. H.; Kortelainen, P.; Caraco, N. F.; Melack, J. M.; Middelburg, J. J. The global abundance and size distribution of lakes, ponds, and impoundments. *Limnol. Oceanogr.* **2006**, *51* (5), 2388−2397.

(23) DelSontro, T.; Kunz, M. J.; Kempter, T.; Wueest, A.; Wehrli, B.; Senn, D. B. Spatial heterogeneity of methane ebullition in a large tropical reservoir. *Environ. Sci. Technol.* **2011**, *45* (23), 9866−9873.

(24) Ortiz-Llorente, M. J.; Alvarez-Cobelas, M. Comparison of biogenic methane emissions from unmanaged estuaries, lakes, oceans, rivers and wetlands. *Atmos. Environ.* **2012**, *59*, 328−337.

(25) Fogler, H. S. *Elements of Chemical Reaction Engineering*; Prentice-Hall; Upper Saddle River, NJ, 1992.

(26) Hanson, P. C.; Bade, D. L.; Carpenter, S. R.; Kratz, T. K. Lake metabolism: Relationships with dissolved organic carbon and phosphorus. *Limnol. Oceanogr.* **2003**, *48* (3), 1112−1119.

(27) Ripp, J. *Analytical Detection Limit Guidance & Laboratory Guide for Determining Method Detection Limits*, PUBL-TS-056-96; Wisconsin

Department of Natural Resources: WI, 1996; http://dnr.wi.gov/regulations/labcert/documents/guidance/-lodguide.pdf.

(28) Bellido, J. L.; Peltomaa, E.; Ojala, A. An urban boreal lake basin as a source of CO_2 and CH_4. *Environ. Pollut.* **2011**, *159* (6), 1649−1659.

(29) Huttunen, J. T.; Alm, J.; Liikanen, A.; Juutinen, S.; Larmola, T.; Hammar, T.; Silvola, J.; Martikainen, P. J. Fluxes of methane, carbon dioxide and nitrous oxide in boreal lakes and potential anthropogenic effects on the aquatic greenhouse gas emissions. *Chemosphere* **2003**, *52* (3), 609−621.

(30) Stocker, T. F.; Qin, D.; Plattner, G.-K.; Tignor, M.; Allen, S. K.; Boschung, J.; Nauels, A.; Xia, Y.; Bex, V.; Midgley, P. M., Eds. *Climate Change 2013: The Physical Science Basis. Contribution of Working Group I to the Fifth Assessment Report of the Intergovernmental Panel on Climate Change*; Cambridge University Press: New York, 2013.

(31) Ouellet, A.; Lalonde, K.; Plouhinec, J. B.; Soumis, N.; Lucotte, M.; Gelinas, Y. Assessing carbon dynamics in natural and perturbed boreal aquatic systems. *J. Geophys. Res.: Biogeosci.* **2012**, *117* (G3), G03024.

(32) Whitfield, C. J.; Aherne, J.; Baulch, H. M. Controls on greenhouse gas concentrations in polymictic headwater lakes in Ireland. *Sci. Total Environ.* **2011**, *410*, 217−225.

(33) Utsumi, M.; Nojiri, Y.; Nakamura, T.; Nozawa, T.; Otsuki, A.; Takamura, N.; Watanabe, M.; Seki, H. Dynamics of dissolved methane and methane oxidation in dimictic Lake Nojiri during winter. *Limnol. Oceanogr.* **1998**, *43* (1), 10−17.

(34) Lennon, J. T.; Faiia, A. M.; Feng, X. H.; Cottingham, K. L. Relative importance of CO_2 recycling and CH_4 pathways in lake food webs along a dissolved organic carbon gradient. *Limnol. Oceanogr.* **2006**, *51* (4), 1602−1613.

(35) Bastviken, D.; Cole, J. J.; Pace, M. L.; Van de Bogert, M. C. Fates of methane from different lake habitats: Connecting whole-lake budgets and CH_4 emissions. *J. Geophys. Res.: Biogeosci.* **2008**, *113* (G2), G02024.

(36) Skaugstad, C.; Behr, A. *Evaluation of Stocked Waters in Interior Alaska 2007*; Fishery Data Series No. 10-90; Alaska Department of Fish and Game: AK, 2010.

(37) Anthony, K. M. W.; Anthony, P. Constraining spatial variability of methane ebullition seeps in thermokarst lakes using point process models. *J. Geophys. Res.: Biogeosci.* **2013**, *118* (3), 1015−1034.

(38) Cole, J. J.; Pace, M. L.; Carpenter, S. R.; Kitchell, J. F. Persistence of net heterotrophy in lakes during nutrient addition and food web manipulations. *Limnol. Oceanogr.* **2000**, *45* (8), 1718−1730.

(39) Berggren, M.; Lapierre, J. F.; del Giorgio, P. A. Magnitude and regulation of bacterioplankton respiratory quotient across freshwater environmental gradients. *ISME J.* **2012**, *6* (5), 984−993.

(40) Wetzel, R. G. *Limnology: Lake and River Ecosystems*; Elsevier Science: CA, 2001.

(41) Walter, K. M.; Chanton, J. P.; Chapin, F. S.; Schuur, E. A. G.; Zimov, S. A. Methane production and bubble emissions from arctic lakes: Isotopic implications for source pathways and ages. *J. Geophys. Res.: Biogeosci.* **2008**, *113* (G2), G00A08.

In situ measurement of dissolved methane and carbon dioxide in freshwater ecosystems by off-axis integrated cavity output spectroscopy

Rodrigo Gonzalez-Valencia,[†] *Felipe Magana-Rodriguez,*[†] *Oscar Gerardo-Nieto,*[†] *Armando Sepulveda-Jauregui,*[‡] *Karla Martinez-Cruz,*[†,‡] *Katey Walter-Anthony,*[‡] *Doug Baer,*[§] *and Frederic Thalasso**[†,‡]

[†]Biotechnology and Bioengineering Department, Cinvestav, Mexico City, D.F., Av. IPN 2508, San Pedro Zacatenco, MX 07360

[‡]Water and Environmental Research Center, University of Alaska Fairbanks, AK 07360

[§]Los Gatos Research, Inc., Mountain View, CA 94041

Supporting information

17 pages (including references)

Extended description of materials and methods.

Figure S1. (A) Peak response of the UGGA to injections of known CH_4 concentrations; (B) Integrated area of the peak response to increasing quantities.

Figure S2. Headspace concentrations in the sampling syringe for several shaking times.

Figure S3. Measured CH_4 concentrations by the M-ICOS after sudden changes in C_{CH4}.

Figure S4. Example of the field response of the M-ICOS method to sudden change in water concentrations and calculated C_{CH4}.

Table S1. Main characteristics of the selected lakes.

Table S2. M-ICOS prototype specifications.

Material and methods

UGGA details

Unlike conventional optical methods that rely on low-resolution spectroscopic techniques (e.g., non-dispersive infrared detectors), the UGGA uses a cavity enhanced laser absorption spectrometry technique that quantifies concentrations, based on measurements of high-resolution absorption lineshapes of the target molecules. The fully resolved lineshapes are recorded by tuning independent telecommunication narrow bandwidth (1 MHz) diode lasers, operating near 1600 nm (CO_2) and 1651 nm (CH_4, H_2O), over 1 cm^{-1} wide spectral windows, respectively, which straddle the target molecular transitions. Real-time spectroscopic analyses of the measured spectra enables a direct continuous determination of the gas concentrations at rates up to 1 Hz, using Beer's Law, and assessments of gas temperature and pressure in the measurement cell. Because of the use of narrow linewidth tunable lasers to record high resolution, fully resolved lineshapes, no instrument deconvolution is required and cross interferences from other compounds are virtually eliminated.[1]

Prototype details

The prototype included a continuous flow of CH_4- and CO_2-free analytical grade nitrogen (Infra, Mexico or Airgas, U.S.A.) and a continuous flow of water extracted at the desired depth from the freshwater ecosystem through a vacuum line (Figure 1). The gas and the liquid crossed at a gas exchange station. The water line (6 mm internal diameter polyurethane tubing) included a suction probe to extract continuously the water sample. This probe consisted of a plastic tubing (25 mm diameter, 50 mm long), filled with a washable polyester wool filter to avoid line-clogging by sediment or suspended particulate matter. The probe was fixed on a thin pole for low depth environments or on a 200 g weight for deeper environments to ensure accurate location at the desired sampling depth. The water flow passed through the gas/liquid exchange station, which consisted of a silicone tubing array (Permselect, PDMSXA-1000, Medarray Inc., USA) and then ended in a vacuum graduated glass container with a vacuum gauge. The vacuum glass container was connected to a portable air sampling pump (PCXR4, SKC, USA) that created a fixed vacuum driving force. The water flow rate through the water sampling line was measured volumetrically several times prior to C_w profile determinations. The water flow rate was also controlled through the determination of t_d. As t_d is a direct function of the water flow rate, t_d was a clear indicator of constant water flow rate. It should be noticed that at each sampling location the M-ICOS method was calibrated against the H-ICOS method. As such, a constant water flow rate at approximately 600 mL min^{-1} was the main factor to ensure precise C_w measurement.

The gas line (6 mm internal diameter polyurethane tubing) included a 27” gas cylinder containing CH_4- and CO_2-free nitrogen (Infra, Mexico or Airgas, U.S.A.). The gas flow rate was regulated at 3 L min^{-1} with a mass flow controller (GFC17, Aalborg, USA). After passing through the gas/liquid exchange station, the air was filtered (AcroVent Filter 0.2 μm, Pall, USA.) twice to avoid condensed water entering the UGGA detector. The complete set-up weighed approximately 30 kg, was powered by a 50 kWh boat battery, and was easily operable by a single person from a small portable boat, although a two-person crew allowed an easier operation.

Details on H-ICOS method

The H-ICOS, described in the main body of the article, is an adaptation of the traditional gas/liquid equilibration technique, where the equilibrium between a water sample and a CH_4- and CO_2-free nitrogen headspace is obtained in a 60-mL sampling syringe. After measuring the syringe's headspace concentration by UGGA, the dissolved gas concentration in the water sample was determined according to Henry's law (eqs S1 and S2), where C_w is the dissolved gas concentration in the water sample (CH_4 or CO_2; mol L^{-1}), C^*_g the gas concentration measured in the headspace of the equilibration syringe (mol L^{-1}); V_l and V_g the water and gas volumes in the syringe, respectively (L); *H'* the CH_4 and CO_2 air/water partition coefficient (-), defined from eq S2; 1.013 is the conversion factor from atm to bars; *R* is the universal gas constant (0.082 L atm K^{-1} mol^{-1}); *T* is the equilibration temperature (K) at the time of measurement; K_H is the Henry's law constant at 298.15 K (1.40x 10^{-3} and 34.0 x 10^{-3} mol L^{-1} bar^{-1}, for CH_4 and CO_2, respectively);[2] and β is the temperature dependence coefficient of the Henry's law constant (1700 and 2400 K, for CH_4 and CO_2, respectively).[2]

$$C_w = \frac{(C^*_g \cdot V_g) + \left(\frac{C^*_g}{H'} \cdot V_l\right)}{V_l} \qquad \text{(S1)}$$

$$H' = \frac{1}{1.013 \cdot R \cdot T \cdot K_H \cdot exp\left[\beta \cdot \left(\frac{1}{T} - \frac{1}{298.15}\right)\right]} \qquad \text{(S2)}$$

Details on the M-ICOS method

The M-ICOS method consisted of a counter flow of CH_4- and CO_2-free nitrogen and water, crossing in the silicone tubing array, as described in the main body of the article. The gas transfer can be described by a diffusion model, according to the Fick's second law (eq 1, repeated here for clarity);

$$\frac{dM}{dt} = 1000 \cdot K \cdot A_M \cdot \left(C_w - \frac{C_g}{H'}\right) \tag{1}$$

Since the transferred gas is directed to the gas phase and since the carrier gas contained no CH_4 and CO_2, eq 1 was modified to eq S3, which was obtained from a simple mass balance, where Q_g is the gas flow rate (L s^{-1}).

$$C_g \cdot Q_g = 1000 \cdot K \cdot A_M \cdot \left(C_w - \frac{C_g}{H'}\right) \tag{S3}$$

By rearranging eq S3, eq S4 is obtained, in which membrane, gas, and water transfer characteristics (Q_g, K, A_M and H') are combined into a single parameter α for easier calculation.

$$C_w = \frac{C_g \cdot Q_g}{1000 \cdot K \cdot A_M} + \frac{C_g}{H'} = C_g \cdot \left(\frac{Q_g}{1000 \cdot K \cdot A_M} + \frac{1}{H'}\right) = C_g \cdot \alpha \tag{S4}$$

Equation S4 shows the direct proportionality between C_w and C_g, which is directly detected by the UGGA, offering a convenient method for the measurement of the dissolved gas concentration. The parameter α can be determined by measuring first C_w by the H-ICOS method and then, with the same sample, by measuring C_g by the M-ICOS. This can be easily done in the field with actual water samples.

An important issue with the M-ICOS method is the delay time (t_d) and the response time (t_r) and of the system, as briefly described in the main body of the article. A continuous flow stirred tank reactor (CSTR) model of hydraulic residence time[3] describes well the hydraulic behavior of the system (eq 3).

$$C_{wm} = C_w \cdot \left[1 - exp\left(-\frac{t}{t_r}\right)\right] \tag{3}$$

By the derivation of eq 3, eq S5 is obtained;

$$C_w = \frac{dC_{wm}}{dt} \cdot t_r + C_{wm} \tag{S5}$$

Taking into account t_d, eq 4 was obtained.

$$C_{w,t} = \frac{dC_{wm,t+t_d}}{dt} \cdot t_r + C_{wm,t+t_d} \tag{4}$$

Laboratory testing

The precision and linearity of the UGGA were tested by injecting several CH_4 and CO_2 standards (from 2, 5, 20, 50, 200, and 500 ppm High Purity Standards, Infra) and by simultaneously measuring these standards with a gas chromatograph. We used a Clarus-500 (Perkin Elmer, USA) chromatograph equipped with a flame ionization detector (FID) detector and an Elite - Q Plot column for CH_4 and a thermal conductivity detector (TCD) and an Alltech Hayesep D 100/120 column for CO_2.

The first test of the H-ICOS method was to establish the peak response of the UGGA to several volumes and CH_4 and CO_2 concentrations injected in the gas line. With this purpose, a continuous CH_4- and CO_2-free nitrogen gas flow rate of 3 L min^{-1} was established and controlled with a mass flow controller; then, 0.1 to 40 mL of 2 to 500 ppm CH_4 or 20 to 500 ppm CO_2 standards were injected. The peaks obtained were integrated (concentration over time using Wolfram Mathematica 8.0, USA). Then, synthetic water samples, containing a known C_w, were prepared in a 3 L lab-scale STR (ez-Control, Applikon, Netherlands) by injecting a continuous flow of 2 to 500 ppm standard gases in 2.5 L tap water with strong mixing (800 rpm), until saturation was obtained. To establish the time required to reach saturation in the STR, prior experiments were conducted by injecting air or nitrogen and measuring the dissolved oxygen concentration until 100% or 0% saturation was obtained (HI2400, Hanna Instruments, USA). Water containing a known dissolved gas concentration was prepared by mixing and gassing times at least two times greater. The dissolved gas concentration in water, with all standards, was established according to Henry's law (eqs S1 and S2). Samples of water were taken with a disposable

60 mL syringe, according to the H-ICOS method, and several shaking times were tested to establish the time required to reach equilibrium between the water sample and the headspace of the syringe. The headspace was injected in the UGGA and also measured by gas chromatography. Then, the M-ICOS method was tested, using the same water samples, in order to establish α (eq 2). Finally, t_d and t_r were determined with the M-ICOS method, by switching between water containing CH_4 and CO_2 to degased water using a 3-way valve. These experiments were also used to check the t_r model developed (eq 4).

Field-testing

The prototype and both methods were tested in four different lakes with contrasting climates, ecologies, and morphologies. The first lake was a eutrophic subtropical reservoir located in the Mexico metropolitan area (Lake Guadalupe, 19.6310 N, 99.2567 W). The second lake was a mesotrophic subtropical reservoir located in the same drainage basin as Lake Guadalupe (Lake Llano, 19.6577 N, 99.5069 W). Both subtropical lakes have been previously described.[4] The third lake was a shallow yedoma-type, thermokarst lake (Lake Goldstream, 64.9156 N, 147.8486 W), and the fourth lake was a shallow non-thermokarst lake (Lake Otto, 63.8413 N, 149.0384 W). Lake Goldstream has been previously described.[5-6] Lake Otto is a shallow tundra lake subject to high winds, which has been hitherto studied.[7]

Statistical and error analysis

The method detection limit (MDL)[8] of both H-ICOS and M-ICOS were determined as the minimum concentration that can be distinguished from background noise with 99% confidence. The goodness of the correlation between the experimental data and the response time model (eq 4) was quantified with the coefficient of determination (R^2). Measurement error was determined by the coefficient of variation, defined as the standard deviation divided by the arithmetic mean, and by the standard error of the mean, defined as the coefficient of variation divided by the square root of the replicate number. We also measured the signal to noise ratio of the UGGA, which is the arithmetic mean of the UGGA reading, divided by the standard deviation. Accuracy was calculated as the absolute difference between the measured and the expected concentration relative to expected concentration. Dynamic range was calculated as the logarithmic ratio between the maximum and the minimum concentrations measured. Maximum concentration was theoretically estimated from the UGGA specifications.

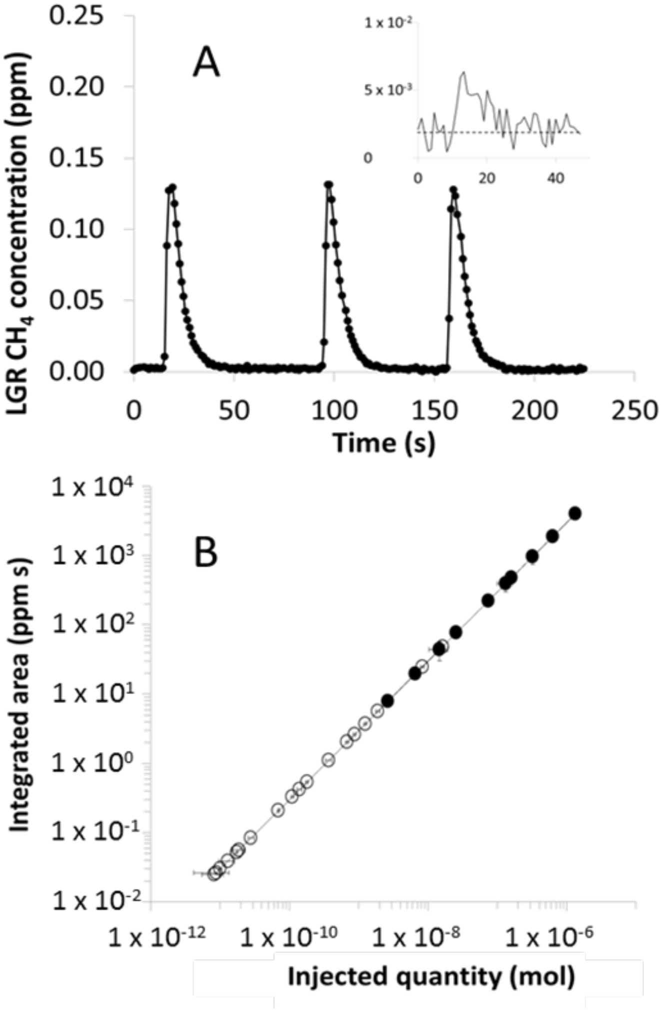

Figure S1. (A) Example of peak response of the UGGA to triplicate injection of 5 mL nitrogen containing 2 ppm of CH_4 and the minimum injected CH_4 quantity that was distinguishable from the background (inner Figure); (B) Integrated area of the peak response to increasing CH_4 (white dots) and CO_2 (black dots) quantities.

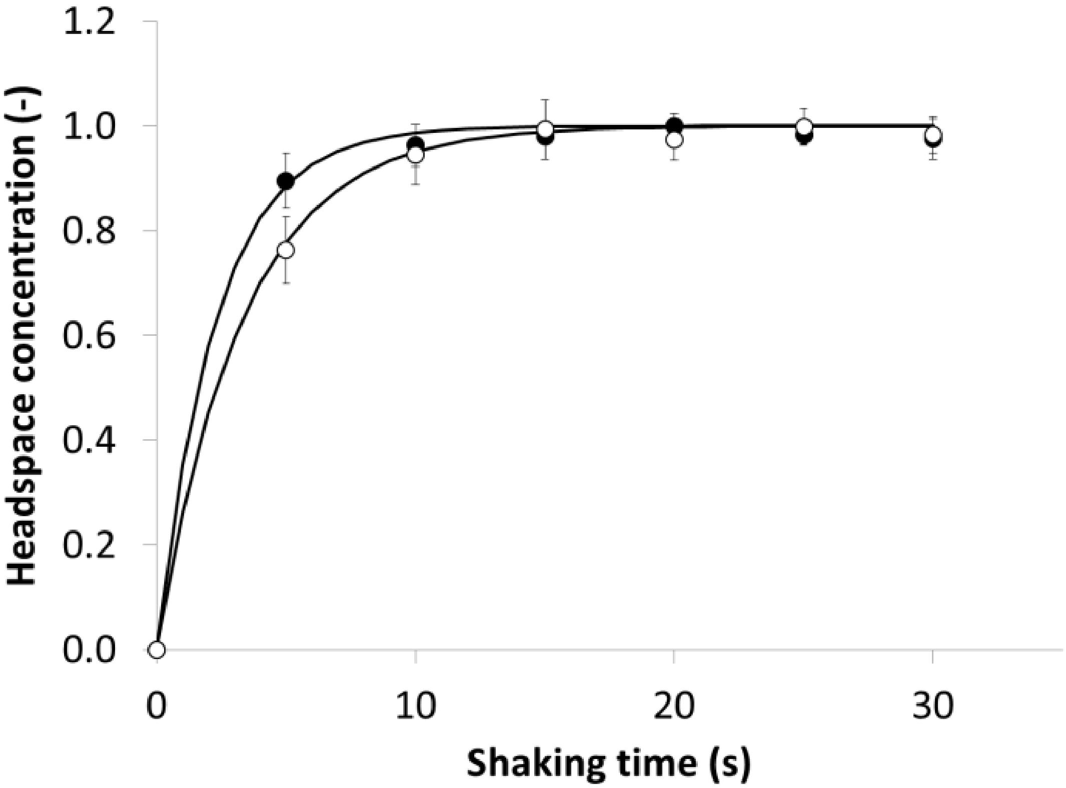

Figure S2. Normalized CH_4 (white dots) and) CO_2 (black dots) headspace concentrations in the sampling syringe for several shaking times. Error bars indicate the standard deviation of the triplicate measurements.

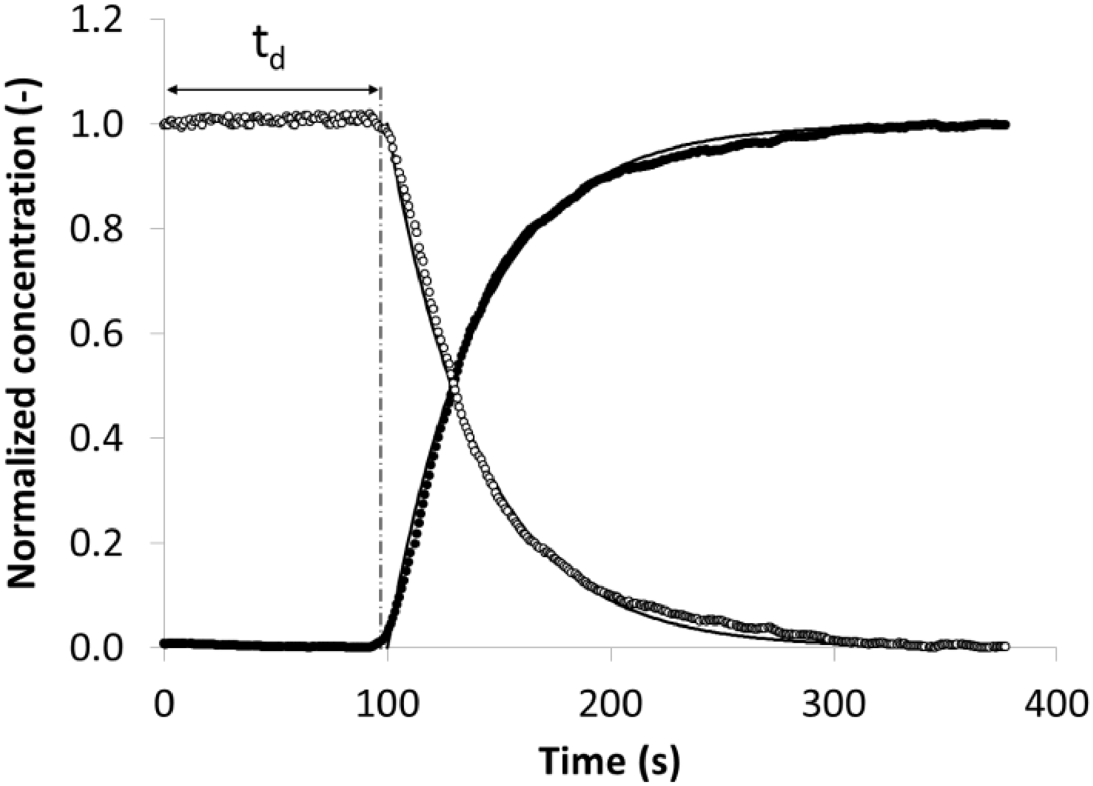

Figure S3. Example of measured CH_4 concentrations by the M-ICOS after sudden changes in C_{CH4}; decreasing concentration gradient (white dots) and increasing concentration gradient (black dots); normalized concentration, 1.0 being the initial or final steady state concentration.

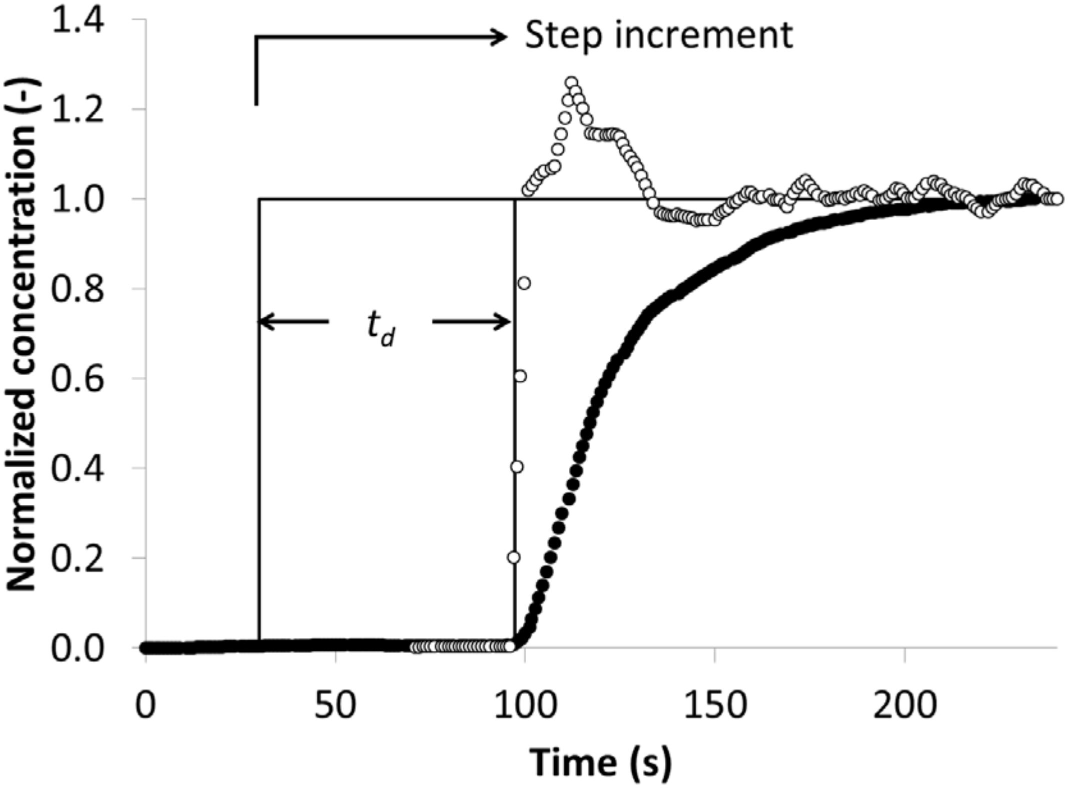

Figure S4. Example of the field response of the M-ICOS method to sudden change in water concentrations (black dots), as well as C_{CH4} calculated from eq 4 (white dots); normalized concentration, 1.0 being the final steady state concentration.

Table S1. Main characteristics of the selected lakes.

Lake	Guadalupe	Llano	Goldstream	Otto
Area (km^2)	4.5	0.06	0.1	0.51
Mean depth (m)	13.3	9.49	3.3	2.5
TSI[a] (-)	Hypereutrophic	Mesotrophic	Distrophic	Oligotrophic
Secchi Depth (m)	0.55	2.13	1.0	1.6
pH	7.2	6.77	7.78	7.68
Surface DO (mg L^{-1})	2.89	6.48	8.50	7.94
Bottom DO (mg L^{-1})	0.00	4.02	0.01	7.93
Surface temperature (°C)	21.75	13.88	18.18	12.46
Bottom temperature (°C)	17.35	11.62	11.62	12.28
Mixed layer[b] (m)	0.50	0.50	1.10	2.5
Temperature gradient in the thermocline[c] (°C m^{-1})	2.80	2.44	3.01	No thermocline

[a] Trophic State Index, measured as given by Carlson.[9]

[b] Layer from the surface of the water to the depth at which temperature declined at a rate lower than 1 °C m^{-1}.

[c] The thermocline was considered to be the layer between the depth at which temperature started to decline at a rate higher than 1 °C m^{-1}, to the depth at which it started to decline at a rate lower than 1 °C m^{-1}.[10]

Table S2. M-ICOS prototype specifications.

Weight (complete prototype)	30 kg
Shipping dimension (suitcase)	0.47 × 0.36 × 0.18 m (UGGA)
Power consumption (external battery)	12 VDC, 5.8 A (70 W)
Operating temperature	0 + 40 °C
Startup time	2 min
Response time UGGA	8 s
Response time M-ICOS	9.77 ± 1.01 s
Calibration time[a]	15 min
Data acquisition frequency	1 Hz
Signal to noise ratio CH_4	1520 ± 415
Signal to noise ratio CO_2	1803 ± 344
Standard error of the mean C_{CH4} determination (n = 100)[b]	0.17 %
Standard error of the mean C_{CO2} determination (n = 100)[b]	0.20 %
Method detection limit C_{CH4}	2.76×10^{-10} mol L^{-1}
Method detection limit C_{CO2}	1.50×10^{-7} mol L^{-1}
Accuracy for CH_4	10.64%
Accuracy for CO_2	12.22%
Dynamic range for CH_4	5.00
Dynamic range for CO_2	5.18

[a] Triplicate calibration with H-ICOS method and determination of t_r and t_d.

[b] n = number of replicates

REFERENCES

(1) Baer, D. S.; Paul, J.B.; Gupta, J.B.; O'Keefe, A. Sensitive absorption measurements in the near-infrared region using off-axis integrated-cavity-output spectroscopy. *Appl. Phys. B-Lasers O.* **2002**, *75* (2-3), 261-65.

(2) Wilhelm, E.; Batino, R.; Wilcock, R.J. Low-pressure solubility of gases in liquid water. *Chem. Rev.* **1977**, *77* (2), 219-262.

(3) Fogler, H. S. *Elements of Chemical Reaction Engineering*; Prentice-Hall; Upper Saddle River, NJ, 1992.

(4) Sepulveda-Jauregui, A.; Hoyos-Santillan, J.; Gutierrez-Mendieta, F. J.; Torres-Alvarado, R.; Dendooven, L.; Thalasso, F. The impact of anthropogenic pollution on limnological characteristics of a subtropical highland reservoir "Lago de Guadalupe", Mexico. *Knowl. Manag. Aquat. Ecosyst.* **2013**, (410); DOI 10.1051/kmae/2013059.

(5) Walter, K. M.; Chanton, J. P.; Chapin, F. S.; Schuur, E. A. G.; Zimov, S. A. Methane production and bubble emissions from arctic lakes: Isotopic implications for source pathways and ages. *J. Geophys. Res Biogeosci.* **2008**, *113* (G2), G00A08.

(6) Anthony, K. M. W.; Vas, D. A.; Brosius, L.; Chapin, F. S.; Zimov, S. A.; Zhuang, Q. L. Estimating methane emissions from northern lakes using ice-bubble surveys. *Limnol. Oceanogr. Meth.* **2010**, *8*, 592-609.

(7) Skaugstad, C.; Behr, A. *Evaluation of Stocked Waters in Interior Alaska 2007*; Fishery Data Series No. 10-90; Alaska Department of Fish and Game: AK, 2010.

(8) Ripp, J. *Analytical Detection Limit Guidance & Laboratory Guide for Determining Method Detection Limits*, PUBL-TS-056-96; Wisconsin Department of Natural Resources: WI, 1996; http://dnr.wi.gov/regulations/labcert/documents/guidance/-lodguide.pdf.

(9) Carlson, R.E. Trophic State Index For Lakes. *Limnol. Oceanogr.* **1977**, *22* (2) (361-369).

(10) Gauthier, J.; Prairie, Y. T.; Beisner, B. E. Thermocline deepening and mixing alter zooplankton phenology, biomass and body size in a whole-lake experiment. *Freshwater Biol.* **2014**, *59* (5), 998-1011.